Eur. Phys. J. C 9, 479–485 (1999)
Digital Object Identifier (DOI) 10.1007/s100529900063

THE EUROPEAN PHYSICAL JOURNAL C

QCD, conformal invariance and the two Pomerons

S. Munier, R. Peschanski

CEA, Service de Physique Theorique, CE-Saclay, F-91191 Gif-sur-Yvette Cedex, France

Received: 8 February 1999 / Revised version: 8 March 1999 / Published online: 18 June 1999

Abstract. Using the solution of the BFKL equation including the leading and subleading conformal spin components, we show how the conformal invariance underlying the leading $\log(1/x)$ expansion of perturbative QCD leads to elastic amplitudes described by two effective Pomeron singularities. One Pomeron is the well-known "hard" BFKL leading singularity, while the new one appears from a shift of the higher conformal spin BFKL singularities from subleading to leading position. This new effective singularity is compatible with the "soft" Pomeron and thus, together with the "hard" Pomeron, meets at large Q^2 the "double Pomeron" solution which has recently been conjectured by Donnachie and Landshoff.

1 Introduction: two Pomerons?

In a recent paper [1] the conjecture was put forward that not one, but two Pomerons could coexist. This proposal is based on a description of data for the proton singlet structure function $F(x,Q^2)$ in a wide range of $x(< 0.7)$ and all available Q^2 values (including also the charm structure function and elastic photoproduction of J/Ψ on the proton). The singlet structure function reads

$$F\left(x,Q^2\right) = \sum_{i=0}^{2} F_i\left(x,Q^2\right) = \sum_{i=0}^{2} f_i\left(Q^2\right) x^{-\epsilon_i}, \quad (1)$$

corresponding [1] to the sum of three contributions, namely a "hard" Pomeron contribution with a fitted intercept $\epsilon_0 = 0.435$, a "soft" Pomeron exchange, as seen in soft hadronic cross sections with a fixed intercept $\epsilon_1 = 0.0808$, and a secondary Reggeon singularity necessary to describe the larger x region with intercept fixed at $\epsilon_2 = -0.4525$. For convenience we here resume the parametrization used in [1]:

$$\begin{aligned} f_0\left(Q^2\right) &= A_0\left(\frac{Q^2}{Q^2+a_0}\right)^{1+\epsilon_0} \\ &\quad \times \left(1 + X\log\left(1+\frac{Q^2}{Q_0^2}\right)\right) \\ f_1\left(Q^2\right) &= A_1\left(\frac{Q^2}{Q^2+a_1}\right)^{1+\epsilon_1} \\ &\quad \times \frac{1}{1+\sqrt{Q^2/Q_1^2}}, \\ f_2\left(Q^2\right) &= A_2\left(\frac{Q^2}{Q^2+a_2}\right)^{1+\epsilon_2}, \end{aligned}$$

$$\begin{array}{lll} \epsilon_0 = 0.418, & \epsilon_1 = 0.0808, & \epsilon_2 = -0.4525, \\ A_0 = 0.0410, & A_1 = 0.387, & A_2 = 0.0504, \\ a_0 = 7.13, & a_1 = 0.684, & a_2 = 0.00291, \\ Q_0^2 = 10.6, & Q_1^2 = 48.0, & \\ X = 0.485. & & \end{array}$$

The "hard" Pomeron is in particular needed to describe the strong rise of F at small x observed at HERA [2]. The key observation of [1] is that the agreement with the data can be obtained by assuming an opposite Q^2 behavior for the two Pomeron contributions in (1). Indeed, for $Q^2 > 10\,\mathrm{GeV}^2$, $f_0(Q^2)$ is increasing and $f_1(Q^2)$ decreasing (the precise parametrizations of [1] are given in a Regge theory framework).

This picture is suggestive of a situation where the "soft" and "hard" Pomerons are not one and the same object, but two separate Regge singularities with rather different intercept and Q^2 behavior. The "hard" Pomeron may be expected to be governed by perturbative QCD evolution equations. Indeed, at small x, a Regge singularity is expected to occur as a solution of the BFKL equation [3] corresponding to the resummation of the leading $(\bar{\alpha}\ln 1/x)^n$ terms in the QCD perturbative expansion, where $\bar{\alpha} = \alpha N_c/\pi$ is the (small) value of the coupling constant of QCD. The intercept value is predicted to be $\epsilon_0 = 4\bar{\alpha}\ln 2$. It is interesting to note that the phenomenological fit for the hard Pomeron in [1] corresponds to a reasonable value for $\bar{\alpha}(\approx 0.15)$. The goal of the present paper is to show that the global conformal invariance of the BFKL equation [4] leads to a natural mechanism generating both the "hard" and "soft" Pomeron singularities.

The plan of the paper is as follows: in Sect. 2, using the BFKL equation and the set of its conformal-invariant components, we exhibit the phenomenon generating sliding singularities. In Sect. 3, we explicitly describe the two Pomeron configuration obtained from the "sliding" mechanism. In Sect. 4 we confront the resulting effective singu-

larities with the parametrization of [1] and discuss some expectations from non-perturbative corrections at small Q^2. Finally, in Sect. 5, we discuss some phenomenological and theoretical implications of our QCD two Pomeron mechanism.

2 The "sliding" phenomenon

Let us start with the solution of the BFKL equation expressed in terms of an expansion over the whole set of conformal spin components [4]. For the structure functions, one may write (using the notation $Y = \ln 1/x$)

$$F\left(Y,Q^2\right) = \sum_{p=0}^{\infty} F_p\left(Y,Q^2\right) = \sum_{p=0}^{\infty} \int_{1/2-\mathrm{i}\infty}^{1/2+\mathrm{i}\infty} \mathrm{d}\gamma \left(\frac{Q}{Q_0}\right)^{2\gamma} \mathrm{e}^{\bar{\alpha}\chi_p(\gamma)Y} f_p\left(\gamma\right), \tag{2}$$

with

$$\chi_p\left(\gamma\right) = 2\Psi\left(1\right) - \Psi\left(p+1-\gamma\right) - \Psi\left(p+\gamma\right) \tag{3}$$

and Q_0, being some scale characteristic of the target (onium, proton, etc.). $\chi_p(\gamma)$ is the BFKL kernel eigenvalue corresponding to the $SL(2,\mathcal{C})$ unitary representation [4] labelled by the conformal spin p. It is to be noted that the $p = 0$ component corresponds to the dominant "hard" BFKL Pomeron. Usually the $p \neq 0$ components, required by conformal invariance[1] but subleading by powers of the energy, are omitted with respect to the leading logs QCD resummation. They are commonly neglected in the phenomenological discussions. We shall see that they may play an important rôle, however.

The couplings of the BFKL components to external sources are taken into account by the weights $f_p(\gamma)$ in (2). Little is known about these functions and we shall treat them as much as possible in a model-independent way. For instance, they should obey some general constraints, such as a behavior when $\gamma \to \infty$ ensuring the convergence of the integral in (2). We will see that some extra analyticity constraints will appear in the context of the two Pomeron problem[2].

The key observation leading to the sliding phenomenon starts by considering the successive derivatives of the kernels $\chi_p(\gamma)$. One considers the following suitable form:

$$\chi_p\left(\gamma\right) \equiv \sum_{\kappa=0}^{\infty} \left\{ \frac{1}{p+\gamma+\kappa} + \frac{1}{p+1-\gamma+\kappa} - \frac{2}{\kappa+1} \right\},$$

$$\chi_p'\left(\gamma\right) \equiv -\sum_{\kappa} \left\{ \frac{1}{\left(p+\gamma+\kappa\right)^2} - \frac{1}{\left(p+1-\gamma+\kappa\right)^2} \right\},$$

$$\chi_p''\left(\gamma\right) \equiv 2\sum_{\kappa} \left\{ \frac{1}{\left(p+\gamma+\kappa\right)^3} + \frac{1}{\left(p+1-\gamma+\kappa\right)^3} \right\}. \tag{4}$$

As is obvious from (4), the symmetry $\gamma \Longleftrightarrow 1-\gamma$ leads to a maximum at $\gamma = 1/2$ for all p, and thus to a saddle point of expression (2) at $\mathrm{Re}(\gamma) = 1/2$ for ultra-asymptotic values of Y. The saddle-point approximation gives

$$F\left(x,Q^2\right)|_{Y\to\infty} \approx \left(\frac{Q}{Q_0}\right) \sum_{p=0}^{\infty} \frac{f_p\left(\frac{1}{2}\right)}{\sqrt{\pi\bar{\alpha}\chi_p''\left(\frac{1}{2}\right)Y}}\, \mathrm{e}^{\bar{\alpha}\chi_p\left(\frac{1}{2}\right)Y}. \tag{5}$$

The Q dependent factor corresponds to a common anomalous dimension $1/2$ for all p. Note that the known Q dependent "k_T diffusion" factor is absent in this ultra-asymptotic limit.

The series of functions of Y is such that only the first term has intercept $\bar{\alpha}\chi_p(1/2)$ larger than 0. Indeed,

$$\chi_0\left(\frac{1}{2}\right) = 4\ln 2 \approx 2.77,$$
$$\chi_1\left(\frac{1}{2}\right) = \chi_0\left(\frac{1}{2}\right) - 4 \approx -1.23,$$
$$\chi_{p+1}\left(\frac{1}{2}\right) < \chi_p\left(\frac{1}{2}\right) < \cdots < 0, \quad p \geq 1. \tag{6}$$

This ultra-asymptotic result is the reason why the conformal spin components with $p > 0$ are generally neglected or implicitly taken into account by ordinary secondary Regge singularities with intercept less than 0. However, at large enough values of Q^2 and even for very large Y, a sliding phenomenon moves away the singularities corresponding to these conformal spin components, leading to a behavior very different from (5). Indeed, the sliding mechanism is already known [6,7] to generate the diffusion factor of the leading $p = 0$ component. However it has an even more important effect on the higher spin components as we shall discuss now.

The sliding mechanism is based on the fact that $\chi_p''(1/2)$, the second derivative of the kernels at the asymptotic saddle-point value, becomes in absolute value very small when $p \geq 1$, in such a way that the real saddle points governing the integrals of (2) are considerably displaced from $\gamma = 1/2$. Indeed, considering the expansions (4), one has

$$\chi_0''\left(\frac{1}{2}\right) = 28\zeta(3) \approx 33.6,$$
$$\chi_1''\left(\frac{1}{2}\right) = 28\zeta\left(3\right) - 32 \approx 1.66,$$

[1] In the following, we will stick to integer values of p since half-integer spin components exist but do not contribute to elastic cross-sections [5].

[2] Note that a general constraint on the coupling of the BFKL kernel to external particles is coming from gauge invariance [4]. We checked that this constraint is rather weak in our case, and not relevant to the discussion.

$$1.66 > \cdots > \chi''_p\left(\frac{1}{2}\right) > \chi''_{p+1}\left(\frac{1}{2}\right) > 0, \quad p \geq 2\ . \qquad (7)$$

For the $p = 0$ component, the corresponding integral in (2) can be evaluated by a saddle point in the vicinity of $\gamma = 1/2$, and gives the diffusion factor $\exp(-\log^2(Q/Q_0)^2/2\bar{\alpha}Y\chi''_0(1/2))$. Considering the rapid decrease by a factor 20 of the modulus of the second derivative for $p = 1$, it is easy to realize that, for components $p \geq 1$, it is no more justified to evaluate the integrals in the vicinity of $\gamma = 1/2$, the real saddle point being away from this value. We shall make the correct evaluation in the next section.

3 The "sliding" mechanism

Let us consider the F_p component of the summation (2) in the following way: For each value of $(Y, \ln(Q^2/Q_0^2))$, we compute the *effective intercept* (in units of $\bar{\alpha}$) $(\partial \ln F_p/\bar{\alpha}\partial Y)$ displayed as a function of the *effective anomalous dimension* $(\partial \ln F_p/\partial \ln Q^2) = \gamma_c$. Our observation is that, for any weight $f_p(\gamma)$ in (2), the resulting set of points accumulates near the curve $\chi_p(\gamma)$. This result is valid provided a saddle point dominates the integral.

The proof goes as follows: If a saddle point γ_c dominates the integral (2) for $F_p(Y, Q^2)$, the saddle-point equation

$$\frac{\partial \ln F_p}{\partial \gamma_c} = 2\ln(Q/Q_0)^2 + \bar{\alpha}Y\chi'_p(\gamma_c) + [\ln f_p(\gamma_c)]' = 0 \qquad (8)$$

is verified and the resulting integral is approximated by

$$F_p(Y, Q^2) \approx \frac{(Q/Q_0)^{2\gamma_c}\, e^{\bar{\alpha}\chi_p(\gamma_c)Y}\ f_p(\gamma_c)}{\left\{2\pi\left(\bar{\alpha}Y\chi''_p(\gamma_c) + [\ln f_p(\gamma_c)]''\right)\right\}^{1/2}}\ . \qquad (9)$$

Neglecting in (9) derivatives of the slowly varying saddle-point prefactor $\{\cdots\}^{-1/2}$, one may write

$$\frac{\mathrm{d}\ln F_p}{\bar{\alpha}\mathrm{d}Y} = \frac{\partial \ln F_p}{\partial \gamma_c} \times \frac{\mathrm{d}\gamma_c}{\bar{\alpha}\mathrm{d}Y} + \frac{\partial \ln F_p}{\bar{\alpha}\partial Y} = \frac{\partial \ln F_p}{\bar{\alpha}\partial Y} \equiv \chi_p(\gamma_c)$$

$$\frac{\mathrm{d}\ln F_p}{\mathrm{d}\ln Q^2} = \frac{\partial \ln F_p}{\partial \gamma_c} \times \frac{\mathrm{d}\gamma_c}{\mathrm{d}\ln Q^2} + \frac{\partial \ln F_p}{\partial \ln Q^2} = \frac{\partial \ln F_p}{\partial \ln Q^2} \equiv \gamma_c, \qquad (10)$$

where one uses the saddle-point equation (8) to eliminate the contributions due to the implicit dependence $\gamma_c(Y, Q^2)$. This proves our statement.

Interestingly enough, the property (10) is valid for any weight $f_p(\gamma)$, and thus can be used to characterize the generic behavior of the expression (2). The only condition is the validity of a saddle-point approximation which is realized whenever Q^2 or Y is large enough.

Let us discuss some relevant examples. In Figs. 1 and 2 we have plotted the result of the numerical integration in expression (2) for $p = 0, 1, 2$, choosing $f_p(\gamma) \equiv 1/(\cos\pi\gamma)/4$. This weight is chosen in such a way that the convergence properties of the integrands are ensured and no extra singularity is generated for $|\gamma| < 2$. Other weights with the same properties were checked to give the same results. For comparison we also display the functions $\chi_0(\gamma), \chi_1(\gamma)$ and $\chi_2(\gamma)$. Note that we have also included for the discussion the auxiliary branches of $\chi_0(\gamma)$ for the intervals $-1 < \gamma < 0$ and $-2 < \gamma < -1$.

The results both for $p = 0$ (white circles) and $p = 1, 2$ (black circles) are displayed in Fig. 1 for a fixed large value of total rapidity $Y = 10$ and various values of $\ln Q^2/Q_0^2$, while in Fig. 2 they are shown for a fixed value of $\ln Q^2/Q_0^2 = 4$ and various Y. Indeed, it is seen on these plots that the saddle-point property (10) is verified, even for the auxiliary branches[3]. The observed small systematic shift of the numerical results with respect to the theoretical curves $\chi(\gamma)$ is well under control. It is related to the saddle-point prefactor in (9).

By various verifications, we checked that the results shown in Figs. 1 and 2 are generic if the following three conditions are realized:
(i) Y or $\ln Q^2/Q_0^2$ are to be large enough ($\geq 2, 3$) to allow for a saddle-point method.
(ii) $f_p(\gamma)$ is constrained to ensure the convergence and positivity of the integrals of expression (2) in the complex plane.
(iii) $f_p(\gamma)$ has no singularity for $\mathrm{Re}(\gamma) > -p$.

The striking feature of the results displayed in Figs. 1 and 2 is that, while remaining in the vicinity of the curve $\chi_p(\gamma_c)$, $\mathrm{d}\ln F_p/\bar{\alpha}\mathrm{d}Y$ and $\mathrm{d}\ln F_p/\mathrm{d}\ln Q^2$ are shifted away from the ultra-asymptotic saddle point at $\gamma = 1/2$. Moreover, the shift is larger if the conformal spin p is higher.

Let us make a particular comment on the analyticity constraint (iii). Obviously, the presence of a singularity at $\mathrm{Re}\gamma > -p$ would prevent the existence of a shift. Indeed, in Fig. 3, we show the result for $f_p(\gamma) = (\gamma\cos\pi\gamma/4)^{-1}$ where we have explicitly violated the constraint (iii) by a pole at $\gamma = 0$. As a result, the components F_1 and F_2, remain still very close to their reference curves $\chi_1(\gamma)$ and $\chi_2(\gamma)$, but they appear "sticked" at the singularity point $\gamma = 0$. Thus the relation (10) remains satisfied, but the sliding mechanism is "frozen" by the singularity, as expected from the analyticity properties.

The main consequence of the sliding mechanism is to substantially modify the evaluation of the sum (2) with respect to the ultra-asymptotic expectation (5). Indeed[4] the situation seen on Figs. 1 and 2 is general: the first contribution F_0 is subject to a rather small shift from $\gamma = 1/2$, while the $p = 1$ component F_1 remains at values where $\mathrm{d}\ln F_1/\bar{\alpha}\mathrm{d}Y$ is slightly above 1 and $\mathrm{d}\ln F_1/\mathrm{d}\ln Q^2$ is be-

[3] In the case of the two auxiliary branches considered in Figs. 1 and 2, we have considered an integration contour shifted by one and two units to the left in order to separate the appropriate contributions from the leading ones.

[4] Using various examples we found this result to be generic provided constraints (i)–(iii) are verified.

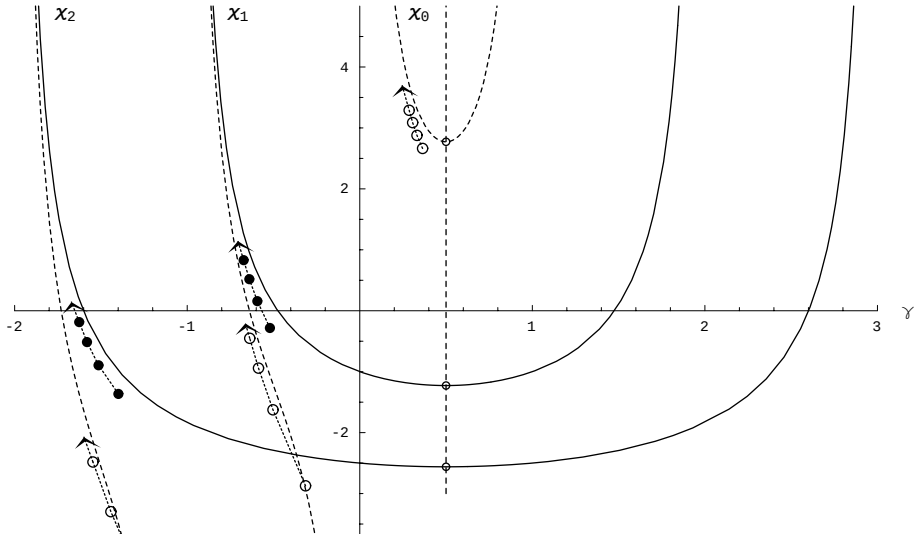

Fig. 1. Plot of effective intercept vs. effective dimension at fixed Y. The effective intercept $\partial \ln F_p/\bar{\alpha}\partial Y$ plotted vs. the effective anomalous dimension $\partial \ln F_p/\partial \ln Q^2$ is compared to the $\chi_p(\gamma)$ functions for the 3 first conformal spin components ($p = 0, 1, 2$). They are computed for a fixed value of $Y = 10$ and 4 values of $\ln Q^2/Q_0^2 = \{4, 6, 8, 10\}$. The chosen weight in the integrals (2), see text, is $f_p(\gamma) = 1/(\cos \pi\gamma/4)$. Black circles: numerical results for $p = 1, 2$ components; white circles: numerical results for the $p = 0$ component computed for 3 different integration contours for $\mathrm{Re}\gamma = 0.5, -0.5, -1.5$; white dots: ultra-asymptotic saddle points at $\gamma = 1/2$; full lines: the functions $\chi_p(\gamma)$ for $(1, 2)$; dashed lines, the function $\chi_0(\gamma)$ including two auxiliary branches. Arrows indicate the direction of increasing Q

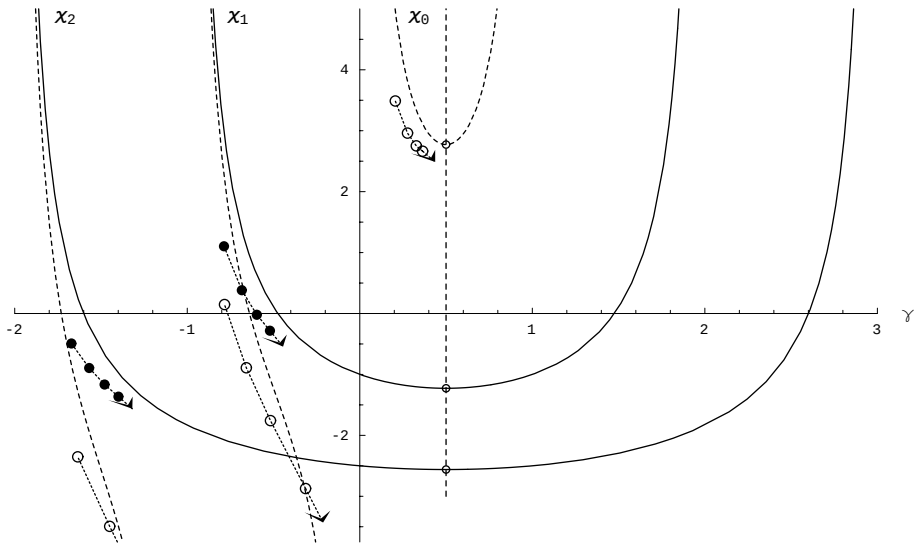

Fig. 2. Plot of effective intercept vs. effective dimension at fixed Q^2. The same as in Fig. 1 but now for fixed $\ln Q^2/Q_0^2 = 4$. The results are computed for $Y = \{4, 6, 8, 10\}$. The arrows describe increasing Y.

low $-1/2$. The higher components F_2 and a fortiori $F_{p>2}$ lie in regions with negative effective intercept and lower and lower values of the effective anomalous dimension.

It is instructive to compare the results of Figs. 1 and 2 for the $p = 1$ component with those obtained for the auxiliary branches of the $p = 0$ one. Though being situated in the same range of effective anomalous dimension γ as the $p = 1$ component, the first auxiliary branch gives sensibly lower (and almost all negative) values of the effective intercept in the kinematical range considered. Thus, the corresponding contributions to the $p = 0$ amplitude are subdominant in energy with respect to the spin 1 amplitude. The same property holds for the second auxiliary branch which stays subdominant with respect to the $p = 2$ component which in any case is itself subdominant with respect to $p = 1$.

Thus, the mechanism we suggest for the two Pomeron scenario is the following: the rôle of the "hard" Pomeron is played (as it should be) by the component F_0, while the rôle of the "soft" Pomeron is played by the other components, principally the component with unit conformal spin F_1. Here this mechanism is realized in a range $(Y, \ln Q^2/Q_0^2)$ where perturbative QCD (with resummation) is valid. Extrapolation to the non-perturbative domain will be discussed in the next section.

4 Physical expectations

It is now worthwhile to discuss our results, obtained from QCD and conformal symmetry, in the context of the phenomenological analysis of [1]. Our goal is not to identify the two approaches, since the theoretical conformal spin expansion (2) is only valid in the perturbative QCD region at large Y and Q^2, while the approach of [1] takes into account the data in the whole range of Q^2. Nevertheless, it is

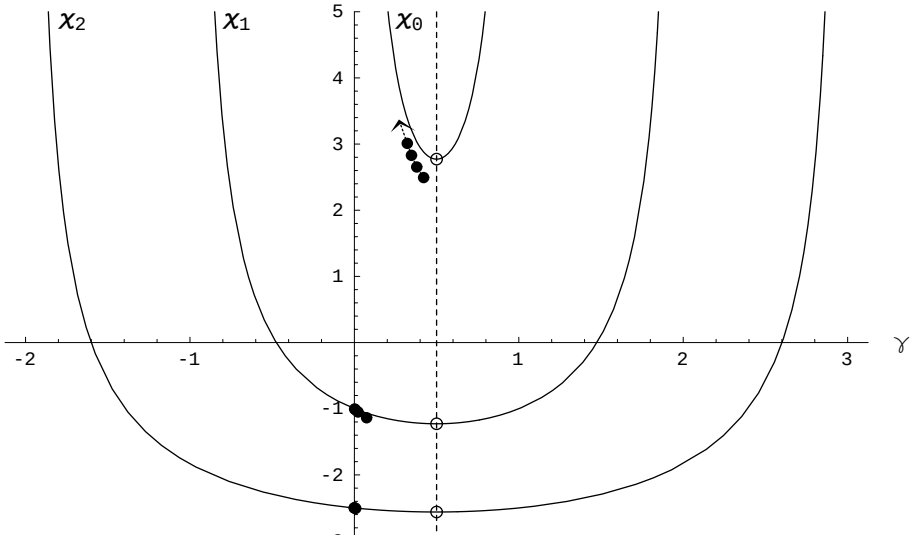

Fig. 3. Plot of effective intercept vs. effective dimension for a singular weight. The plot is the same as Fig. 1 with a weight $f_p(\gamma) \propto 1/(\gamma \cos \pi\gamma/4)$, i.e. singular at $\gamma = 0$. Note the accumulation of black circles near the singularity at $\mathrm{Re}\,\gamma = 0$ for $p = 1, 2$.

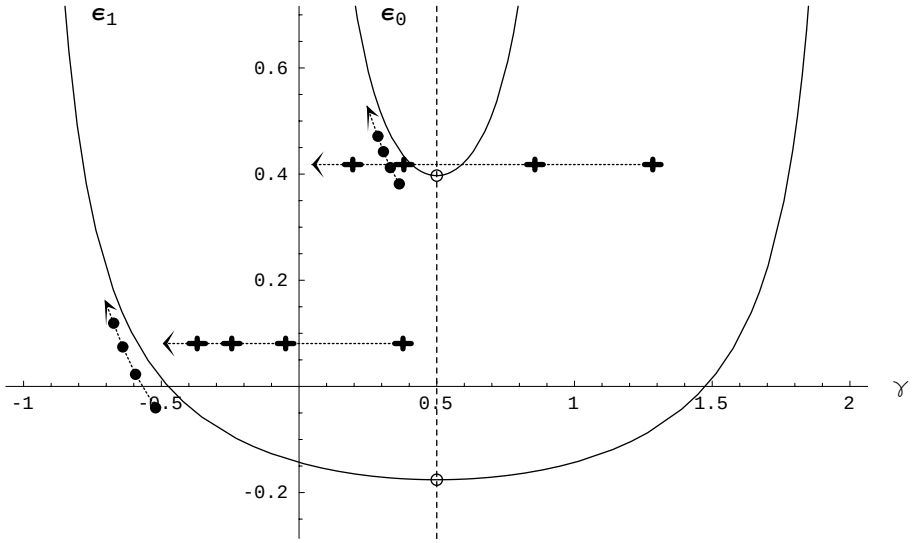

Fig. 4. Comparison with [1]. The plot is similar to Fig. 1, except for a rescaling of the vertical coordinate $Y \to \bar{\alpha}Y$, with $\bar{\alpha} = 0.15$. The curves denoted $\epsilon_{0,1}$ correspond to the same rescaling of $\chi_{0,1}(\gamma)$. The black circles correspond to our calculations at fixed $Y = 10$ and $\ln Q^2/Q_0^2 = (4, 6, 8, 10)$. The results for [1] corresponding to the same values of Y and $\ln Q^2/Q_0^2$ are given by crosses. The arrows indicate the direction of increasing Q^2.

interesting to confront our resulting effective parameters with those obtained from the description of [1].

In Fig. 4 we show a plot comparing our results with those obtained from the two Pomeron components of [1] in terms of the effective parameters as previously. In the case of the parametrization of paper [1], the effective intercept and anomalous dimension are easily identified as, respectively, ϵ_i and $\mathrm{d}\ln f_i(Q^2)/\mathrm{d}\ln Q^2$, see (1). In order to make contact with phenomenology, we have fixed $\bar{\alpha} = 0.15$, and $Q_0 = 135\,\mathrm{MeV}$. This last value is somewhat arbitrary but corresponds to rather high values of $\ln(Q/Q_0)^2$ in the physical range, justifying the existence of a significant saddle point. In practice, in Fig. 4, we have considered $Y = 10$ and $\ln(Q/Q_0)^2 = (4, 6, 8, 10)$. The crosses in Fig. 4 correspond to the effective parameters extracted from the parametrization [1] and the black dots to our numerical results of the integrals (2) for the same values of the kinematical variables. We performed the calculation with $f_p(\gamma) \propto 1/(\cos \pi\gamma/4)$, but checked the validity of the results for other weights (with similar analyticity properties, cf. Sect. 3.)

The main thing to be noticed is the reasonable agreement between both results for large values of Q^2 corresponding to the direction of the arrows on the figure. A few remarks are in order:

(i) The leading "hard Pomeron" singularity obtained by our results is of the type used e.g. in the phenomenological description of proton structure functions in the dipole model of BFKL dynamics [7]. However the value of the coupling constant, chosen here to match with the determination of the hard component by [1], is larger than in one Pomeron fits [7] and in better agreement with the original BFKL framework.

(ii) The nonleading singularity is obtained in the correct range fixed by [1] to be given by the "soft" Pomeron [8]. It is to be remarked that, while the "hard" Pomeron singularity is mainly fixed by the choice of $\bar{\alpha}$, the nonleading one is a result of the sliding mechanism. We thus find this feature to be model independent and related to the

asymptotic conformal invariance of the input amplitudes. (iii) As also seen in the figure, the agreement is not quantitative, especially at lower Q^2, since the results obtained from our (2) appear as *moving* effective singularities while those from paper [1] are, by definition, *fixed* Regge singularities.

Let us comment further on this important difference. In perturbative QCD, there being obeyance to a renormalization group property, one expects in rather general conditions a scale-dependent evolution, different from the Regge-type of singularities, at least for the singlet channel [9] [5]. It is thus not surprising that the various components obtained from our approach show this characteristic feature, see Figs. 1, 2, 3 and 4. On the contrary, pure Regge singularities will correspond to fixed intercepts as shown in Fig. 4 by the horizontal lines.

We feel that moving effective singularities will remain a typical feature of the "hard" singularity at high Q^2, at least if perturbative QCD is relevant in this case. The situation is obviously different for the "soft" singularity the intercept of which is fixed at the known "universal" value for soft interactions [8]. The behavior of the "soft" singularity when Q^2 becomes small is not determined in our perturbative approach. It only predicts that it will become dominant when Q^2 will approach and decrease below Q_0^2, as indicated by the effective anomalous dimension. Non-perturbative QCD effects could thus be expected to stabilize the perturbative soft singularity at the known location of the phenomenological soft Pomeron[6]. Moreover, one would have to consider also the other higher conformal spin components.

Some qualitative arguments can be added in favor of specific non-perturbative effects for conformal spin components. Indeed, the same reason leading to the sliding mechanism, namely the smallness of $\chi_p''(\gamma)$ in the vicinity of $\gamma = 1/2$, implies a large "k_T diffusion" phenomenon [6]. One typically expects a range of "k_T diffusion" for the gluon virtuality scales determining the spin component F_p depending on p as $(\chi_p''(1/2))^{-1}$. Thus, while the contamination of non-perturbative unitarization effects could be limited for F_0, it is expected to be strong for F_1 and the higher spin components $F_{p>1}$. All in all, it is a consistent picture that the softer components obtained in a perturbative QCD framework at high Q^2 are precisely those for which stronger "k_T diffusion" corrections are expected. To go further would require a study of the low-Q^2 region, in particular of higher-twist contributions, which are outside the scope of our present paper[7].

Concerning the physical meaning of the analyticity constraints imposed on the integrand factors $f_p(\gamma)$: they amount to the need to discuss the conformal coupling of the BFKL components to, say, the virtual photon and the proton (or, more generally, other projectiles/targets). Leaving for future work the complete derivation of the conformal couplings to different conformal spins [13,14], let us assume that the coupling is spin independent. Interestingly enough an eikonal coupling to a $q\bar{q}$ pair [15] then appears to be forbidden, since it has a pole at $\gamma = 0$, corresponding to the presence of the gluon coupling in the impact factor [16]. However, considering the direct coupling through the probability distribution of a virtual photon in terms of $q\bar{q}$ pair configurations [17], we remark, following the derivation of [16], that the pole due to the gluon coupling is cancelled with no other singularity at $\gamma = 0$. We explicitly checked that we obtain results very similar to those displayed in Figs. 1, 2 and 3 within this framework. Note that such a model ensures the positivity of the conformal spin contributions.

In our derivation, which follows from the conformal invariance of the BFKL equation, we have sticked to the case of a fixed coupling constant. It has been proposed [4,18, 19] that the solution of the BFKL equation, once modified in order to take into account a running coupling constant, leads to two, or more probably, a series of Regge poles instead of the j plane cut obtained originally at fixed $\bar{\alpha}$. However, this solution with more than one Pomeron singularity does not ensure the specific Q^2 behavior required by the analysis of [1] and obtained by the sliding mechanism. The running of the coupling constant, and more generally the results of the next-to-leading BFKL corrections [20], modify the singularity structure but could preserve the sliding mechanism. Further study is needed in this respect.

5 Conclusion and outlook

To summarize our results, using the full content of solutions of the BFKL equation in a perturbative QCD framework, and in particular their conformal invariance, we have looked for the physical consequences of the higher conformal spin components of the conformal expansion on the problem of the Pomeron singularites. We have found, under rather general conditions, that the obtained pattern of effective singularities leads to two Pomeron contributions, one "hard", corresponding to the ordinary conformal spin 0 component and one "soft", corresponding to higher spin contributions, mainly spin 1. This situation agrees, at least in the large Q^2 domain, with the empirical observation of [1] leading to a "hard" Pomeron with leading-twist behavior and a "soft" Pomeron with higher-twist behavior. It is interesting to note that the higher-twist behavior we obtain corresponding to the $p = 1$ component is of higher effective intercept than the one which may be associated with the auxiliary branches of the "hard" component $p = 0$. Thus, there is no doubt that the $p = 1$ component behavior is emerging from the other secondary BFKL contributions. However, its order of magnitude remains to be discussed [14].

It is important to note that the higher spin components rely on the existence of an asymptotic global conformal

[5] Note, however, the different perturbative approach of [10].

[6] Another possibility [11] could be a pole in the weight $f_p(\gamma)$ at a suitable position, but this would not be easily justified by a physical property like e.g. conformal invariance.

[7] The known studies on higher-twists effects at low x [12] seem to show a behavior different from the one obtained from the sliding mechanism of higher conformal spin components. This feature certainly deserves further study.

invariance. This invariance has been proved to exist in the leading-log approximation. In the next-to-leading log BFKL calculations, it has recently been advocated [21] to be preserved, at least approximately. If this result is confirmed, and if the characteristics of the kernels are similar, the rôle of the modified higher conformal spin components is expected to be the same. Further tests of our conjecture also imply a study of the specific couplings of the higher spin components to the initial states and an extension of the predictions to the non-forward diffractive scattering. Indeed, it has recently been shown [22] that the photoproduction of J/Ψ gives evidence for no shrinkage of the Pomeron trajectory. Thus the two Pomeron conjecture could also be borne out by considering non-forward processes.

If confirmed in the future, the two Pomeron conjecture leads to further interesting questions, for instance:
(i) Can we built an Operator Product Expansion for the structure functions, and thus higher-twist contributions, incorporating the conformal invariance structure?
(ii) Can we get some theoretical information on the physical "soft" Pomeron by considering high-Q^2 indications given by perturbative QCD indications?
(iii) Can we see some remnants of the specific conformal spin structure associated with the two Pomerons?
(iv) The sliding mechanism appears as a kind of a spontaneous violation of asymptotic conformal invariance: can we put this analogy in a more formal way?

One interesting conclusion to be drawn from our study is that the matching of hard and soft singularities could be very different from expectation. Usually, it is expected that a smooth evolution is obtained from the hard to the soft region thanks to the increase of the unitarity corrections to some "bare" Pomeron. By contrast, in the empirical approach of [1] and in the theoretical sliding mechanism discussed in the present paper, the "hard" and "soft" regions are essentially dominated by distinct singularities, with only small overlap. Clearly, this alternative deserves further phenomenological and theoretical studies. In particular, there have been suggestions [11] to extend the study to (virtual) photon–photon reactions where the perturbative singularities and their specific coupling are expected to be theoretically well defined. For instance, if the eikonal coupling is confirmed as a characteristic feature of the (virtual) photon coupling to the BFKL kernel, the sliding mechanism should not work for the spin 1 component and thus the would-be "soft" Pomeron is expected to be absent from these reactions. Another case study is the Pomeron in hard diffractive reactions where the sliding mechanism, if present, could be different than for total structure functions, and thus might lead to a different balance of hard and soft singularities.

Acknowledgements. We want to thank the participants of the Zeuthen Workshop on DIS at small x, ("Royon meeting", june 1998) for fruitful discussions, among whom Jeff Forshaw, Douglas Ross for stimulating remarks and particularly Peter Landshoff for provoking us with his and Donnachie's conjecture. We are also indebted to Andrzej Bialas and Henri Navelet for interesting suggestions and comments.

References

1. A. Donnachie, P.V. Landshoff, Phys. Lett. B **457**, 408 (1998), hep-ph/9806344
2. H_1: C. Adloff et al., Nucl. Phys. B **497**, 3 (1997); ZEUS: D. Breitweg et al., Phys. Lett. B **407**, 432 (1997)
3. L.N. Lipatov, Sov. J. Nucl. Phys. **23** (1976) 642; V.S. Fadin, E.A. Kuraev, L.N. Lipatov, Phys. Lett. B **60** (1975) 50; E.A. Kuraev, L.N. Lipatov, V.S. Fadin, Sov.Phys.JETP **44**, 45 (1976), **45** (1977) 199; I.I. Balitsky, L.N. Lipatov, Sov.J. Nucl.Phys. **28** (1978) 822
4. L.N. Lipatov, Zh. EKsp. Teor. Fiz. **90** (1986) 1536 [Sov. Phys. JETP **63** (1986) 904]
5. H. Navelet, S. Wallon, Nucl. Phys. B **522**, 237 (1998)
6. J. Bartels, H. Lotter, Phys. Lett. B **309**, 400 (1993)
7. H. Navelet, R. Peschanski, Ch.Royon, S. Wallon Phys. Lett. B **385**, 357 (1996)
8. A. Donnachie, P.V. Landshoff, Phys. Lett. B **296**, 227 (1992)
9. A. de Rújula et al., Phys. Rev. D **10**, 1649 (1974)
10. C. Lopez, F. Barreiro, F.J. Yndurain, Zeit. für Phys. C **72**, 561 (1996), and references therein
11. A. Bialas, private communication
12. J. Bartels, Nucl. Phys. (Proc. Suppl.) B **71**, 47 (1999), Sect. 3, (Proceedings of Multiparticle Dynamics 1997, edited by Frascati, G. Capon, V.A. Khoze, G. Pancheri, A. Sansoni), and references therein
13. H. Navelet, R. Peschanki, Nucl. Phys. B **515**, 269 (1998)
14. N. Marchal, R. Peschanki, hep-ph/9905378
15. A.H. Mueller, W.-K. Tang, Phys. Lett. B **284** (1992) 123; J. Bartels et al., Phys. Lett. B **348**, 589 (1995)
16. S. Munier, R. Peschanki, Nucl. Phys. B **524**, 377 (1998)
17. N.N. Nikolaev, B.G. Zakharov, Zeit. für Phys. C **49**, 607 (1991)
18. M. Braun, G.P. Vacca, G. Venturi, Phys. Lett. B **388**, 823 (1996)
19. N.N. Nikolaev, B.G. Zakharov, V.R. Zoller, JETP Lett. (1997) 138; Pisma Zh. Eksp. Teor. Fiz. **66**, 134 (1997)
20. V.S. Fadin, L. Lipatov, Phys. Lett. B **429**, 127 (1998); G. Camici, M. Ciataloni, Phys. Lett. B **430**, 349 (1998)
21. S.J. Brodsky, V.S. Fadin, V.T. Kim, L.N. Lipatov, G.B. Pivovarov, hep-ph/9901229
22. A. Levy, Phys. Lett. B **424**, 191 (1998)